



## PSHA TESTING AGAINST HISTORICAL SEISMICITY EXAMPLE OF FRANCE

P. Labbé

Professor, Ecole Spéciale des Travaux Publics, Cachan, France, plabbe@estp-paris.eu

### **Abstract**

In order to test PSHA outputs against historical seismicity data, the seismic risk is first introduced in terms of annual probabilities of occurrence of given damage degrees for vulnerability class B buildings (EMS98 scale). Then the risk is calculated from two methods. The first one considers historical earthquakes of epicentral Intensities  $I_0 = VI$  to IX, and statistics of affected areas. The second one is based on convolution of seismic hazard and fragility curves. Seismic hazard is described by the SHARE map of the metropolitan France. Fragility curves are described in the form of a log-normal distribution of the probability of exceedance of a given damage versus the PGA, according to the recent results of the SYNER-G European research program. The risk calculated on the basis of the SHARE map and fragility curves is tremendously higher, by a factor of 100, than the historically observed risk. Some tracks are discussed on the origin of this gap, on ways to bridge it and on further uses of PSHA testing.

*Keywords: PSHA testing; Historical seismicity; Hazard map; Seismic risk; Fragility curves.*

### **1. Introduction**

Probabilistic seismic hazard assessment (PSHA) is a more and more popular technique for establishing hazard maps at the scale of a country or even at a much larger scale. However, it appears that PSHA techniques are not yet mature enough to provide outputs that are reasonably insensitive to expert judgements. The case of France exemplifies this lack of maturity: three different maps were established, in 2002, 2004 and 2006, leading to a huge variability in the hazard assessment of the metropolitan France [1]. Consistency of these 3 maps against historical seismicity was already presented by the author in 2010 [1]. More recently a new map of seismic hazard was proposed as an output of the European research program SHARE [2] (Fig. 1). The purpose of this paper is to discuss the consistency of the SHARE map against historical seismicity, taking also into account the more recent developments on fragility curves resulting from the SYNER-G European research program [3].

Different authors proposed some approach for testing PSHA outputs against historical seismicity. For instance a counting process of exceedance of a given threshold on a series of site can be implemented [4], with due consideration for the limits of such metrics [5]. For the purpose of testing, it is preferable that PSHA outputs consider also rather short return periods (such as 100 or 200 years), although these return periods are not necessary for the final user of the PSHA [6]. Testing PSHA outputs requires in principle that a large number of sites is considered so as to compensate for a relatively short period of observation on every individual site by independent observations on numerous sites, in an (implicit) ergodic assumption [7]. Concurrently it is of course obvious that a single event is not meaningful for PSHA testing [8]. Reliability of the historical data could also be questioned and possible biases in intensity data be examined [9], but it is not our purpose in this paper where intensity data are regarded as an input.

When testing PSHA outputs against historical seismicity, a general feature of the proposed methods is that, at a given moment, it is necessary to translate macroseismic observations into accelerations (generally PGA). This is not the case for the method that we present in this paper, which is based on seismic risk



assessment. The seismic risk is defined as the probability that a vulnerability class B building (representative of conventional masonry building) experiences a damage grade D according to the definitions of the European Macroseismic Scale (EMS98) [10]. Consistently with the seismic risk exposure in the metropolitan France the damage grades 2 to 4 (D=2, 3, 4) are considered in this paper.

Then the core of the method consists of calculating the seismic risk by two different approaches:

- The first one derives the risk from historical seismicity. It is based on a statistical analysis of both earthquakes felt in France and isoseismical maps.
- The second one calculates the risk by convolution of hazard maps and fragility curves.

Finally the two risk estimates are compared and conclusions are drawn about consistency of the SHARE hazard map with historical seismicity.

## 2. Seismic risk based on historical seismicity

### 2.1. Areas yearly affected by a given intensity

#### 2.1.1. Principle of calculation

We consider a territory with a seismic activity homogeneous (in space) and stationary (in time). Taking the example of intensity VI, we denote  $A_{VI}$  the average area of this territory yearly affected by intensity equal to or larger than VI. Conceptually, would we have at our disposal comprehensive macro-seismic data on a very long period of time (T years), calculating  $A_{VI}$  would be easily achieved as follows: For every event  $i$ , occurring during the period of time T, we denote  $\mathcal{A}_{i,VI}$  the area affected by an intensity larger than or equal to VI. Then

$$A_{VI} = \mathcal{A}_{VI}/T \quad \text{with} \quad \mathcal{A}_{VI} = \sum \mathcal{A}_{i,VI} \quad (1)$$

Practically we do not have at our disposal the above-mentioned ideal comprehensive information. However, taking the example of the French territory, we can build on historical data as follows: We denote

- $n_{I_0}$  ( $I_0 \geq VI$ ) the number of events of epicentral intensity  $I_0$ , felt in France during a reference period of time T, practically one century.
- $A_{I_0,VI}$  the average area affected by an intensity larger than or equal to VI for an event of epicentral intensity  $I_0$ .

Then an estimate of  $\mathcal{A}_{VI}$  is given by Eq. (2). It can be introduced into Eq.(1) to get an estimate of  $A_{VI}$ . Other  $A_I$  can be estimated similarly.

$$\mathcal{A}_{VI} = \sum n_{I_0} A_{I_0,VI}, \quad I_0 = VI \text{ to IX} \quad (2)$$

#### 2.1.2 Application to the metropolitan France

On the basis of available data, the period of time 1895-1994 has been selected as the best documented, representative of a century of seismicity. In particular, events with an epicentre out of the French territory and felt in France are reported by Lambert *et al.* [11] and Sisfrance [12], and counted in the Table 1 (numbers are rounded-up).

Table 1 : Average number of events ( $I_0 \geq VI$ ) felt per century in the metropolitan France

Epicentral Intensity, $I_0$	VI	VI-VII & VII	VII-VIII & VIII	VIII-IX
Number of events, $n_{I_0}$	90	70	10	1

For the purpose of calculating  $A_{I_0,VI}$  values, an atlas of 140 isoseismical maps, compiled by Levret *et al.* [13], was processed. We do not present in this paper the detail of the statistical processing. A major output is that, for a given epicentral intensity, isoseismal areas are log-normally distributed. Average values of these areas are presented in the Table 2.



Table 2 : Average area affected by an intensity  $\geq VI$  for a given epicentral intensity

Epicentral Intensity, $I_0$	VI	VI-VII & VII	VII-VIII & VIII	VIII-IX
Average affected area (km <sup>2</sup> )	52	1040	5200	31700
Inside France	33	680	1620	1810

Applying the Eq. (2) formula with data included in the Tables 1 and 2 leads to:  $A_{VI} = 689 \text{ km}^2$  for the metropolitan France. The same procedure leads to results presented in the second line of the Table 3 for other intensities.

### 2.1.3. Variability of seismic activity in the territory

Of course seismic activity cannot be regarded as homogeneous inside the metropolitan French territory. Therefore, in the frame of this study, the territory is divided into three zones on the basis of the French administrative map of “Départements” and the number of epicentral intensities VI observed per “Département” [12] (Figure 2). The zone areas are indicated in the Table 3 as well as the percentage of activity (percentage of epicentral intensities VI observed in the zone compared to the total number in the territory). For the three zones, areas affected by intensities VI to IX are reported in the Table 3.

Table 3. Average annual areas (km<sup>2</sup>) affected by a given intensity (or higher) on the basis of historical seismicity

	VI	VII	VIII	IX
French metropolitan territory, 544690 km <sup>2</sup>	689	60	3.5	0.4 (*)
Zone 1, 87 170 km <sup>2</sup> , 16 % territory, 80 % activity	589	56	3.5	0.4
Zone 2, 241 260 km <sup>2</sup> , 44 % territory, 16 % activity	89	4	0	0
Zone 3, 216 260 km <sup>2</sup> , 40 % territory, 4 % activity	11	0	0	0

(\*) Assumed value in the absence of historical data.

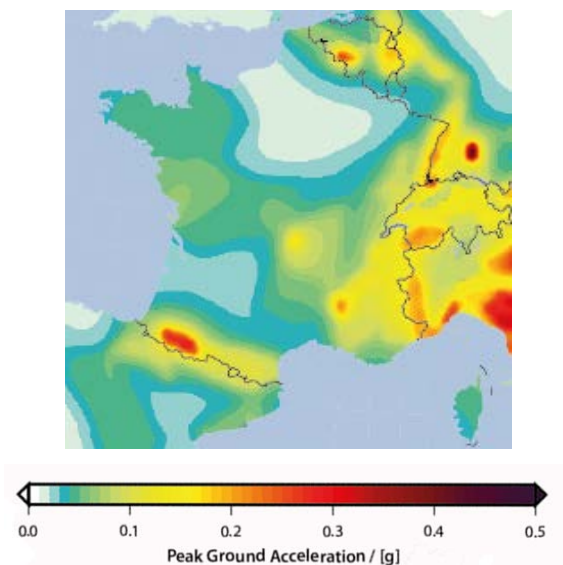


Fig. 1 excerpt of SHARE map (475 y., rock)

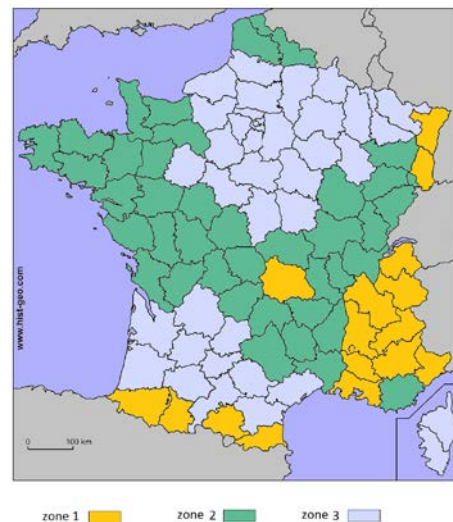


Fig. 2 Zonation based on historical seismicity



## 2.2 Annual probability of damage grade 2 to 4 for vulnerability class B buildings

The EMS98 scale [10] classifies types of buildings according to their sensitivity to seismic input motion and introduces a definition of damage grades. According to this scale, and considering the vulnerability class B, the proportion of buildings that undergo grade 2 to 4 damage is related to the intensity as reported in the Table 4. Definitions of terms *a few*, *many* and *most* are based on fuzzy set techniques. They lead to quantify the terms as follows: *a few* is equivalent to 8%, *many* to 35% and *most* to 80%.

Table 4 : Damage rate vs Intensity for vulnerability class B buildings according to EMS 98

Intensity	VI	VII	VIII	IX
D=2 (damage grade 2)	a few	many	<i>most</i>	<i>all</i>
D=3 (damage grade 3)	/	a few	many	<i>most</i>
D=4 (damage grade 4)			a few	many

*In italic: interpretation of EMS 98 macroseismic scale*

For calculating the probability that a building undergoes a given damage grade, the probability it is exposed to a given intensity should first be established. This probability is directly derived from data presented in the Table 3. For instance the annual probability that a building located in Zone 1 is exposed to an intensity VII or higher is calculated as  $56 / 87\ 170 = 6,4 \cdot 10^{-4}$ .

Eventually, the annual probability that a vulnerability class B building experiences a given damage grade is calculated. Results are presented in the Table 5.

Table 5 : Annual probability that a vulnerability class B building undergoes a damage grade 2 to 4 (D=2, 3, 4) on the basis of historical seismicity data

	D=2	D=3	D=4
Zone 1	$7.3 \cdot 10^{-4}$	$6.4 \cdot 10^{-5}$	$4.5 \cdot 10^{-6}$
Zone 2	$3.4 \cdot 10^{-5}$	$1.4 \cdot 10^{-6}$	/
Zone 3	$4.1 \cdot 10^{-6}$	/	/

## 3. Seismic risk based on hazard maps and fragility curves

### 3.1. Methodology

#### 3.1.1 Principle of calculation

In the present framework, it is assumed that seismic hazard is described in the form of a map providing Peak Ground Acceleration (PGA) values,  $a_{ref}$ , associated to a given return period,  $T_{ref}$ . On any site of the territory, the annual probability that the observed PGA is greater than  $a$  is denoted  $P_e(a)$ . Consequently the annual probability that a PGA with a value comprised between  $a$  and  $a+da$  occurs on this site is equal to  $p_e(a) da$ , so that :

$$p_e(a) da = - P_e'(a) da \quad (3)$$

Regarding a given type of buildings, its fragility is described by the probability it suffers a damage of degree D (or larger) in case it undergoes a seismic input motion whose PGA equals to  $a$ . This conditional



probability is denoted  $P_{f,D}(a)$ . The annual probability that a building of the considered type suffers a damage of degree  $D$  (or larger) is derived as follows:

$$p_D = \int_0^{\infty} p_e(a) P_{f,D}(a) da . \quad (4)$$

### 3.1.2. Forms of $P_e$ et $P_{f,D}$ functions

It is generally accepted that, at a given location in the territory, return periods,  $T$ , and associated PGAs,  $a$ , are linked by a function of the form given by Eq. (5), where  $T_{ref}$  is the return period selected for establishing the considered hazard map and  $a_{ref}$  the corresponding PGA at the considered location.

$$T/T_{ref} = (a/a_{ref})^n \quad (5)$$

Additionally,  $P_e(a)$  is linked to the return period by  $P_e(a)=1-\exp(-1/T(a))$ , which results in the approximate  $P_e(a) \approx 1/T(a)$  for relatively rare events. Consequently a good approximate of  $P_e(a)$  reads as per Eq. (6), this formula being not applicable for relatively small  $a$  values. A simple derivation leads to the  $p_e(a)$  expression presented in Eq. (7). In practice the selected return period is 475 years, and consequently  $P_e(a)$  takes the form of Eq. (6').

$$P_e(a) = \frac{1}{T_{ref}} \left( \frac{a_{ref}}{a} \right)^n \quad (6)$$

$$p_e(a) = \frac{n}{T_{ref}} \frac{1}{a} \left( \frac{a_{ref}}{a} \right)^n \quad (7)$$

$$P_e(a) = \frac{1}{475} \left( \frac{a_{475}}{a} \right)^n \quad (6')$$

It is also generally accepted that building fragility is log-normally distributed. It means that the population of PGAs generating a damage grade greater than or equal to  $D$  is log-normally distributed; its median value is denoted  $a_D$  and  $\beta_D$  the standard deviation of its natural logarithm.

$$P_{f,D}(a) = \Phi \left[ \frac{1}{\beta_D} \text{Ln} \left( \frac{a}{a_D} \right) \right] \quad \text{with} \quad \Phi(u) = \frac{1}{\sqrt{2\pi}} \int_{-\infty}^u \exp(-t^2 / 2) dt \quad (8)$$

### 3.1.3. Risk analytical formula

On the basis of these assumptions, it is possible to calculate an analytical formula of  $p_D$  given by Eq. (9), which in practice takes the form of Eq. (9').

$$p_D = \frac{1}{T_{ref}} \left( \frac{a_{ref}}{a_D} \right)^n k_D \quad , \quad k_D = \exp \frac{n^2 \beta_D^2}{2} \quad (9)$$

$$p_D = \frac{1}{475} \left( \frac{a_{475}}{a_D} \right)^n k_D \quad , \quad k_D = \exp \frac{n^2 \beta_D^2}{2} \quad (9')$$



This formula should be handled with care. It results from the integral of Eq. (4) with a  $p_e$  expression that is not valid for small  $a$  values. Thus the calculated integral is correct only in case  $P_{f,D}$  is practically nil for these small  $a$  values. In practice it means that  $a_D$  should be large enough so that this condition is met. The author carried out numerical integration tests to guarantee that errors in the presented results are lower than 5%.

### 3.2. Application to the metropolitan France

#### 3.2.1. Hazard data

An evenly distributed grid of 148 sites is used to sample the part of the SHARE map corresponding to metropolitan France. The vast majority (96 %) of sampled  $a_{475}$  values are in the range 0.015-0.15 g, with an average value of 0.054 g. This value can be compared to those obtained from different maps and reported in [1]. Regarding  $n$ , it varies in the SHARE map from values as low as 1.5 in quiet areas, such as Parisian Bassin to 3.5 in the most active areas, such as the Pyreneans.

The 148 sites are distributed into 3 subsets so as to constitute 3 zones according to the following criteria: Zone a is corresponding to  $a_{475} > 0.085$  g, Zone c to  $a_{475} < 0.036$  g, while Zone b is intermediate. Zone a is corresponding to 16% of the territory, Zone b 44% and Zone c 40%. These proportions are basically equal to those of the above introduced Zones 1, 2 and 3. As it can be observed by comparison of Fig. 1 and Fig. 2, there is a good match between Zones 1, 2, and 3 on the one hand and Zones a, b and c on the other hand. The only significant difference is that Corsica appears in Zone 3 on the basis of historical seismicity while it belongs to Zone b on the basis of the SHARE map.

#### 3.2.2 Ground type factors

The SHARE map provides PGA values in rock conditions. It should therefore be taken into account that most of the French territory does not consist of rocky sites. Data on site categorization as per the Eurocode 8 ground types [14] are seldom. A map of  $V_{s,30}$  values is however published by USGS [15], which covers most of the French territory. On this basis, it can be estimated that, in average, a ground type B is representative of site conditions in Zones 1 and 2, while a ground type C is representative in Zone 3. According to Eurocode 8, and taking into account that, in France, the 475 year return period hazard is controlled by low magnitude earthquakes ( $M_S < 5.5$ ) the SHARE hazard values should consequently be amplified by a factor 1.35 in Zones a and b, and a factor 1.5 in Zone c. These amplification factors are adopted in the present study.

#### 3.2.3. Fragility data

In section 2.2, the seismic risk was calculated for buildings of the vulnerability class B. Therefore, in order to obtain a reliable comparison with the output of historical seismicity approach, the fragility curve of class B buildings should now be selected for convolution with the seismic hazard. According to Lagomarsino and Cattari [16] two possible sets of fragility curves can be used, depending on the in-field experience feedback processed either by Murphy and O'Brien [17] (source 1) or more recently by Faccioli and Cauzzi [18] (source 2). Every set includes three curves corresponding to  $D=2, 3$  and  $4$ , whose  $a_D$  and  $\beta_D$  values are reported in the Table 6.

Table 6 :  $a_D$  and  $\beta_D$  values for vulnerability class B

	D=2		D=3		D=4	
	$a_D$ (g)	$\beta_D$	$a_D$ (g)	$\beta_D$	$a_D$ (g)	$\beta_D$
Source 1, [16] & [17]	0.118	0.62	0.204	0.61	0.355	0.63
Source 2, [16] & [18]	0.145	0.54	0.240	0.54	0.390	0.56



### 3.2.4. Calculated risk

Eventually the risk is calculated according to Eqn. (9') at every site of the grid and averaged per zone. The final outputs are presented in the Table 7.

Table 7: Annual probability that a vulnerability class B building undergoes a damage grade 2 to 4 (D=2, 3, 4) on the basis of the SHARE map and fragility data

	Source 1, [16] & [17]			Source 2, [16] & [18]		
	D=2	D=3	D=4	D=2	D=3	D=4
Zone a	/	/	$1.5 \cdot 10^{-3}$	/	$3.0 \cdot 10^{-3}$	$7.1 \cdot 10^{-4}$
Zone b	$2.3 \cdot 10^{-3}$	$5.6 \cdot 10^{-4}$	$1.4 \cdot 10^{-4}$	$9.8 \cdot 10^{-4}$	$2.7 \cdot 10^{-4}$	$8.4 \cdot 10^{-5}$
Zone c	$5.2 \cdot 10^{-4}$	$1.7 \cdot 10^{-4}$	$5.7 \cdot 10^{-5}$	$2.8 \cdot 10^{-4}$	$1.0 \cdot 10^{-4}$	$4.0 \cdot 10^{-5}$
/ case for which formula (9') is regarded as not accurate enough (see § 3.1.3).						

Results presented in the Table 7 should be read as follows: For instance, in Zone b ( $0.036 \text{ g} < a_{475} < 0.085 \text{ g}$ ) the annual probability that a vulnerability class B building undergoes a damage grade D=3 is calculated at  $5.6 \cdot 10^{-4}$  on the basis of Source 1, while it is  $2.7 \cdot 10^{-4}$  on the basis of Source 2. Although they vary by a factor of 2, these two probabilities are of the same order of magnitude. They are comparable to the same annual probability that a vulnerability class B building undergoes a damage grade 3 in Zone 2, which is calculated at  $1.4 \cdot 10^{-6}$  only on the basis of historical seismicity (Table 5).

### 3.2.5. Sensitivity studies

For the purpose of sensitivity studies on the above output, the case {D=3, Zone b}, associated with the fragility data of Source 2 ( $a_{D=3}=0.24$ ,  $\beta_{D=3}=0.54$ ), is selected as reference case and designated as Case 0. As reported in the Table 7 it is corresponding to  $\text{Prob}(D=3, \text{Zone b})=2.7 \cdot 10^{-4}$ .

According to formula (9'), the output is depending on two independent parameters only: the ratio  $A_{\text{ref}}/a_D$  and the product  $n\beta$ . Thus three sensitivity studies are carried out:

- Case 1:  $A_{\text{ref}}/a_D$  is divided by 2, corresponding to  $(A_{\text{ref}}/a_D)'/(A_{\text{ref}}/a_D)=0.5$  in the Table 8.
- Case 2:  $n\beta$  is amplified by 1.5, corresponding to  $(n\beta)'/(n\beta)=1.5$  in the Table 8.
- Case 3 is the combination of Cases 1 and 2.

For the three cases the annual probability that a vulnerability class B building situated in Zone b undergoes a damage grade D=3 is recalculated. The ratio between the new value,  $\text{Prob}'(D=3, \text{Zone b})$ , and the Case 0 is presented in the last line of the Table 8. It can be observed that Case 1 leads to reducing the calculated risk by a factor 6 ( $\text{Prob}'/\text{Prob}=0.17$  in the Table 8), while Case 2 has a minor impact of only 16 %. Case 3 has a stronger impact than expected on the basis of the separate effects of Case 1 and Case 2.

Table 8 – Sensitivity study of risk assessment

	Case 0	Case 1	Case 2	Case 3
$(A_{\text{ref}} / a_D)' / (A_{\text{ref}} / a_D)$	1	0.5	1	0.5
$(n\beta)' / (n\beta)$	1	1	1.5	1.5
$\text{Prob}'(D=3 \text{ Zone b}) / \text{Prob}(D=3 \text{ Zone b})$	1	0.17	0.84	0.056



## 4 Comparisons and conclusions

Comparison of Tables 5 and 7 leads to the conclusion that the seismic risk calculated on the basis of the SHARE map and fragility curves overestimates the historically observed risk by a factor of the order of 100! Several reasons could be put forward in order to explain such a large gap and tracks could be investigated in order to try to bridge the gap.

Risk evaluation on the basis of historical seismicity could be underestimated. In the atlas of isoseismal maps [13] there are only 24 maps with epicentral intensity VI, while 90 events are expected per century. A systematic analysis of macroseismic observations for all events  $I_0 \geq VI$  on a century is on progress in France so as to get a comprehensive set of isoseismal maps and derive a more reliable risk estimate. However it is expected that the events that are already presented in [13] are the best documented and concurrently the more significant so that the re-evaluated risk should likely be lower than estimated at the moment. This should increase the gap between approaches instead of reducing it.

Translation of intensity data into probabilities of damage on the one hand, and fragility curves on the other hand have been carefully selected so that they are consistent, corresponding in both cases at the same vulnerability class. The same exercise could be run by selecting another vulnerability class; it is not expected that the final output be significantly different.

There is certain variability in the fragility curves. However the two options considered in this paper lead to a factor of 2 only in the final risk estimate. A dramatically different assumption is not realistic because fragility data already published by other authors are comparable to those used in the present paper.

The SHARE map is the input data that should be regarded as the main cause of the discrepancy between the two risk calculations. The sensitivity study presented in the Table 8 leads to the conclusion that the seismic hazard presented by SHARE is at least overestimated by a factor 2. This conclusion is consistent with recent seismic hazard re-evaluation in two neighbouring countries of France, Switzerland [19] and Germany [20]. For instance the SHARE map indicates that the 475 year return period PGA is comprised between 0.25 and 0.30 g at Basel city while Swiss and German experts conclude independently that it should be 0.1 g. Similarly along the Rhine graben, the SHARE map indicates 0.16-0.2 g while the estimate of GFZ [20] is 0.06-0.07 g.

Additionally it is possible that the  $n$  values of the SHARE map are underestimated. Values as low as 1.5 (even lower in some parts of Europe) are very questionable. The sensitivity study reported in the Table 8 shows that, when associated to a reduction of the hazard by a factor 2, a 50 % increase of  $n$  values has a significant impact on risk assessment.

In conclusion, in the light of the observed historical seismic risk, the SHARE map tremendously overestimates the seismic hazard in metropolitan France, at least by a factor 2. This conclusion is consistent with the most recent seismic hazard assessments carried out in Switzerland and in Germany. Consequently the SHARE map, as it is at the moment, cannot be regarded as a reliable description of the seismic hazard in metropolitan France.

## 5 Perspectives

Beyond the particular case of the SHARE map and the seismic hazard assessment in the metropolitan France, there are promising perspectives in the use of PSHA testing as a powerful tool to reduce uncertainties in probabilistic seismic hazard assessment. The mathematical background is the Bayes theorem and the associated Bayesian updating technique. This technique is already widely used in several fields of engineering and could be developed as well in the framework of PSHA studies. In its implementation, the weights of the logic tree branches in the PSHA would not be anymore attributed by experts but would be mathematically selected so as to optimize the consistency of PSHA outputs with in-field observations. An example of PSHA Bayesian updating is presented by Secanell *et al.* [21]. In-field observations can be instrumental, historical as developed in the present paper, or based on paleo-data such as precarious rocks [22] or in cave concretions [23]. An international workshop on PSHA testing and benefit of Bayesian techniques for PSHA was recently hosted by the Pavia



University [24]. A conclusion of the workshop is that “A state-of-the-art PSHA should include a testing phase against any available observation, including any kind of observation and any period of observation, including instrumental seismicity, historical seismicity and paleoseismicity data if available”. For countries or regions where sufficient historical data are available, the PSHA testing method presented in the present paper could be used in order to reduce PSHA output uncertainties by the way of the Bayesian updating technique.

#### 4. Acknowledgements

Gloria Senfaute is sincerely acknowledged for her support in processing SHARE map data.

#### 5. References

- [1] Labbé P (2010): PSHA outputs versus historical seismicity; Example of France. *14<sup>th</sup> European Conference on Earthquake Engineering*, Ohrid, FYROM.
- [2] [www.share-eu.org](http://www.share-eu.org)
- [3] Pitilakis K, Crowley H, Kaynia AM (2014): *SYNER-G: Typology Definition and Fragility Functions for Physical Elements at Seismic Risk*, Springer.
- [4] Albarello, D., and V. D’Amico (2008). Testing probabilistic seismic hazard estimates by comparison with observations: An example in Italy, *Geophys. J. Int.* 175, 1088–1094.
- [5] Stein, S., Spencer, B. D., and Brooks, E. M. (2015). “Metrics for Assessing Earthquake Hazard Map Performance.” *Bulletin of the Seismological Society of America*, 105(4), 2160–2173.
- [6] Stirling, M. W., and M. Petersen (2006). Comparison of the historical record of earthquake hazard with seismic-hazard models for New Zealand and the continental United States, *Bull. Seismol. Soc. Am.* 96, 1978–1994.
- [7] Ward S. N. (1995), Area-Based Tests of Long-Term Seismic Hazard Predictions, *Bull. Seismol. Soc. Am.* 85, No. 5, 1285-1298.
- [8] Iervolino, I. (2013). Probabilities and fallacies: Why hazard maps cannot be validated by individual earthquakes, *Earthq. Spectra* 29, no. 3, 1125–1136.
- [9] Hough, S. E. (2013). Spatial variability of “Did You Feel it?” intensity data: Insights into sampling biases in historical earthquake intensity distributions, *Bull. Seismol. Soc. Am.* 103, 2767–2781.
- [10] Grunthal G (1998): *European Macroseismic Scale*, *Cahiers du Centre Européen de Géodynamique et de Séismologie, vol 15*, Luxembourg.
- [11] Lambert J, Levret-Albaret A (1996). *Mille ans de séismes en France*, Ouest éditions, Nantes.
- [12] SisFrance (2013). *Catalogue des séismes français métropolitains*, BRGM, EDF, IRSN, [www.sisfrance.net](http://www.sisfrance.net)
- [13] Levret A, Cushing M, Peyridieu G (1996). Recherche des caractéristiques de séismes historiques en France, Atlas de 140 cartes macrosismiques, IPSN internal report, France.
- [14] Eurocode 8 (2005). Design of structures for earthquake resistance; Part 1: General rules, seismic actions and rules for buildings. AFNOR (French standard institute).
- [15] <http://earthquake.usgs.gov/hazards/apps/vs30/predefined.php>
- [16] Lagomarsino S, Cattari S (2014) *Fragility Functions of Masonry Buildings*, in *SYNER-G: Typology Definition and Fragility Functions for Physical Elements at Seismic Risk*, Springer.
- [17] Murphy JR, O’Brien LJ (1977) The correlation of peak ground acceleration amplitudes with seismic intensity and other physical parameters. *BSSA*, 67:877-915.



- [18] Faccioli E, Cauzzi C (2006). Macroseismic intensities for seismic scenarios, estimated from instrumentally based correlations. *First European Conference on Earthquake Engineering and Seismology*, Geneva.
- [19] [http://www.seismo.ethz.ch/eq\\_swiss/Erdbebengefaehrdung/Karten/Gefaehrdung/index\\_EN](http://www.seismo.ethz.ch/eq_swiss/Erdbebengefaehrdung/Karten/Gefaehrdung/index_EN)
- [20] GeoForschungsZentrum (GFZ), Erbeben-Modell D2015, Personal communication.
- [21] Secanell R, Martin Ch, Viallet E, Senfaute G (2015). A Bayesian methodology to update the Probabilistic Seismic Hazard Assessment. *CSNI Workshop on Testing PSHA Results and Benefit of Bayesian Techniques for Seismic Hazard Assessment*, Eucentre Foundation, Pavia, Italy.
- [22] Anderson JG, Brune JN, Purvance M, Biasi G, Anooshehpour A (2011). Benefits of the use of precariously balanced rocks and other fragile geological features for testing the predictions of probabilistic seismic hazard analysis; in *Applications of Statistics and Probability in Civil Engineering*, Taylor & Francis, London, pages 744-752.
- [23] Gribovszki K, Bokelmann G, Szeidovitz Gy, Paskaleva I, Brimich L, Kovács K, Mónus P (2013) Comprehensive investigation of intact, vulnerable stalagmites to estimate an upper limit on prehistoric horizontal ground acceleration. *Recent Advances in Earthquake Engineering and Structural Dynamics Conference VEESD 2013*, Vienna.
- [24] OECD-NEA (2015) Proceedings of the CSNI Workshop on *Testing Probabilistic Seismic Hazard Analysis Results and the Benefits of Bayesian Techniques*, Pavia, NEA/CSNI/R(2015)15